



# Size-dependent magnon modes of a Heisenberg ferromagnet

To cite this article: S. Cojocaru and A. Ceulemans 2003 *EPL* **61** 838

View the [article online](#) for updates and enhancements.

## You may also like

- [The two-magnon spectrum for the Heisenberg ferromagnet with NN interactions on a square lattice](#)  
M Hood and P D Loly
- [Quantum kink in the continuous one-dimensional Heisenberg ferromagnet with easy plane: a picture of the antiferromagnetic magnon](#)  
K Nakamura and T Sasada
- [Gauge equivalent structures of the integrable \(2+1\)-dimensional nonlocal nonlinear Schrödinger equations and their applications](#)  
Xiaoming Zhu

## Size-dependent magnon modes of a Heisenberg ferromagnet

S. COJOCARU<sup>1,2</sup> and A. CEULEMANS<sup>1</sup>

<sup>1</sup> *Division of Quantum Chemistry, University of Leuven  
Celestijnenlaan 200F, B-3001 Leuven, Belgium*

<sup>2</sup> *Institute of Applied Physics - Chişinău, Moldova*

(received 21 May 2002; accepted 9 January 2003)

PACS. 75.10.Jm – Quantized spin models.

PACS. 75.30.Ds – Spin waves.

**Abstract.** – We prove the existence of new bound magnon excitations in Heisenberg ferromagnets due to finite-size effects. To describe these effects, we develop an analytical approximation which is a modification of the widely used continuum approach. Thus, for the square lattice we find 4 branches of bound two-magnon excitations in addition to the two ones known before. It is shown that some of the new modes remain well separated from all the others even for a macroscopic system.

Presently, there exists a growing interest in finite systems inspired by the variety of qualitatively new properties on meso- and nano-scale (see, *e.g.*, [1]). Although theoretical knowledge about such systems mostly comes from numerical simulations, it is necessary to develop analytical approaches which could provide a better understanding of the mechanisms involved. In the present paper we consider “the simplest” problem, excitations in the isotropic Heisenberg spin-(1/2) ferromagnet with nearest-neighbour interaction, to prove analytically the existence of new modes due to magnon interaction and finite size,  $N$ . More specifically, we focus on bound states as being representative of the essential features of the general many-body problem. On the other hand, bound excitations are relevant for different response functions of a crystal at low temperatures (susceptibility, Raman scattering, ferromagnetic resonance etc.). Recently, the interest in this model has increased as its two-dimensional (2D) version describes the spin excitations of quantum Hall systems at filling factor  $\nu = 1$  [2]. We develop an approximation which allows to capture some important finite-size features and is a modification of the continuum method widely used in condensed matter for the description of the thermodynamic limit  $N \rightarrow \infty$ . It builds upon the preliminary study [3] of a simple 1D system for which one can rely on Bethe’s exact solution [4]. Although the known results obtained by the previous continuum treatments are in agreement with available exact solutions (see [5–7] and [8,9]), some aspects important for finite-size systems have been overlooked. For instance, the single eigenenergy branch of the bound two-magnon state in 1D coincides with Bethe’s famous solution for the finite chain [4] in the thermodynamic limit. However, even for the 1D case the wave function has not been obtained explicitly within the continuum approach and the point

that there should be *two orthogonal* solutions according to Bethe did not receive any comment. Even more puzzling is the situation for higher-dimensional lattices where no exact results are available to compare with, although, according to the cited references, there should be, *e.g.*, two and three bound modes for the square and the simple cubic lattices, respectively. These questions might seem irrelevant since the finite-chain solution predicts only a small difference ( $\sim 1/N^2$ ) in energy between the two excitations showing up at long wavelengths ( $\sim \sqrt{N}$ ). One then expects that the finite-size corrections should become even less relevant for higher dimensions. Surprisingly, quite the opposite turns out to be the case, as we prove below, and the approach of the limit can become rather slow, *e.g.*, logarithmic for the 2D case. It will become clear that the properties of the wave function are essential for this behaviour. We show that the construction of the proper continuum limit requires that the symmetry of the wave functions is explicitly taken into account. This allows to describe the distribution of all the two-magnon modes in the Brillouin zone. For instance, we recover the “lost” second mode of Bethe’s exact solution for the chain and reveal 4 additional modes for the square lattice.

We first show how the main features of Bethe’s exact solution can be described within the framework of a modified continuum approach. Since the total momentum of the excitation  $\mathbf{P}$  is a conserved quantity, it is convenient to consider the amplitude of the two-magnon excitation  $a(n_1, n_2)$  in terms of the “center of mass”  $\mathbf{R}$  and relative  $\mathbf{r}$  coordinates of the flipped spins (*e.g.*, for the 2D case,  $\mathbf{R}_x = (n_2^x + n_1^x)/2$ ,  $\mathbf{r}_x = (n_2^x - n_1^x)$ , etc.). We further adopt Bethe’s convention of numbering the lattice sites so that the relative coordinates  $r_x (= X)$  and  $r_y (= Y)$  are nonnegative integers  $0, 1, \dots, N-1$ . Thus,

$$a(n_1, n_2) = \frac{\exp[i\mathbf{P} \cdot \mathbf{R}]}{N_0^{1/2}} a(\mathbf{r})$$

and the Schrödinger equation leads to [8]

$$[\varepsilon - zJ]a(\mathbf{r}) + J \sum_{\mathbf{d}} \cos\left(\frac{\mathbf{P} \cdot \mathbf{d}}{2}\right) a(\mathbf{r} + \mathbf{d}) = J(\mathbf{r}) \left[ a(\mathbf{0}) \cos\left(\frac{\mathbf{P} \cdot \mathbf{r}}{2}\right) - a(\mathbf{r}) \right], \quad (1)$$

where the sum runs over the  $z$  nearest neighbors,  $\varepsilon$  is the excitation energy and  $J(\mathbf{r}) = J$  for nearest neighbours and zero otherwise. Some symmetry requirements follow from permutation of overturned spins ( $a(\mathbf{r}) = a(-\mathbf{r})$ ) and from cyclic boundary conditions ( $a(n_1^x, n_1^y; n_2^x, n_2^y) = a(n_1^x, n_1^y; n_2^x + N, n_2^y) = a(n_1^x + N, n_1^y; n_2^x, n_2^y)$ , etc.). Taking the square lattice as an example,  $N_0 = N \times N$ , we get

$$a(r_x, r_y) = \exp\left[\frac{iP_x N}{2}\right] a(r_x \pm N, r_y) = \exp\left[\frac{iP_y N}{2}\right] a(r_x, r_y \pm N). \quad (2)$$

As the components of the total momentum take on the values  $2\pi l_x/N$  and  $2\pi l_y/N$  with  $l_x$  and  $l_y$  being integer quantum numbers, existence of eigenstates with even ( $s$ ) and odd ( $a$ ) parity immediately follows from (2) depending on the parity of  $l$ . We then expand the amplitude of the relative motion into the Fourier series:

$$a(\mathbf{r}) = \frac{1}{N_0} \sum_{\mathbf{Q}} b(\mathbf{Q}) \exp[i\mathbf{r} \cdot \mathbf{Q}]. \quad (3)$$

Due to the constraints on the variable  $\mathbf{Q}$  in (3) imposed by (2), we get the relations  $1 = \exp[iN(\frac{P_{x,y}}{2} \pm Q_{x,y})]$  which determine the range of values for the respective components of  $\mathbf{Q}$ :

$$Q_{x,y}^s = \frac{2\pi m}{N}, \quad Q_{x,y}^a = \frac{2\pi m}{N} + \frac{\pi}{N}; \quad m = 0, 1, \dots, N-1. \quad (4)$$

Thus, for the antisymmetric excitation the sequence of values of  $Q_{x,y}^a$  in (3) is shifted as compared to the symmetric  $Q_{x,y}^s$ . Then the Fourier amplitude  $b(\mathbf{Q})$  and the eigenenergy are obtained from (1). As we intend to construct a continuum approximation which would keep track of the symmetry properties of the underlying finite lattice, we have to incorporate the above distinction between the two types of states in our approximation. Therefore we replace the sums by integrals over the *shifted* interval of momenta [3], *i.e.*

$$\frac{1}{N} \sum_{Q^a} \longrightarrow \frac{1}{\pi} \int_{\pi/N}^{\pi+\pi/N} dQ.$$

In this way also the volume of the phase space is preserved. Then we indeed obtain two different branches in the continuum limit for the 1D problem as predicted by Bethe. The single branch mentioned above (see, *e.g.*, [6,8]) corresponds to the symmetric solution  $\varepsilon_s = J \sin^2(\frac{p}{2})$ , while the antisymmetric branch is described by the equation

$$1 - \frac{2 \sin(\frac{\pi}{N})}{\pi \cosh v} = \frac{2(\cosh v - \cos(p/2))}{\pi \sinh v} \arctan\left(\frac{\sinh v}{\sin(\frac{\pi}{N})}\right), \quad (5)$$

where  $v = \text{arccosh}((1 - \varepsilon_a/2J)/\cos(\frac{p}{2}))$  and  $p$  is a continuous variable meant to interpolate between the discrete momenta. As was shown earlier, our approximation reproduces well the exact results [3]. For instance, at the border of the Brillouin zone  $\varepsilon_a = \varepsilon_s = J$ . Towards the long-wavelength region the energy of the antisymmetric excitation grows higher than that of the symmetric one, their separation being scaled as  $p^4$  for small momenta. Both solutions lie below the continuum of scattered magnon states until the latter is crossed by  $\varepsilon_a(p)$  at some critical momentum  $p_c \simeq \frac{2\pi}{\sqrt{N}}$  which should be compared to the value found by Bethe  $P_c^B \simeq \frac{4}{\sqrt{N}}$ . From eq. (5) one can see that it predicts a continuous real-valued eigenenergy solution beyond the crossing point, in the region of the continuum of scattered states  $\varepsilon_a > 2J(1 - \cos(\frac{p}{2}))$ , till exactly the last allowed value of momentum is reached at  $p = 2\pi/N$ . This might seem to be in contradiction with Bethe's treatment which predicts that the bound state exists only below the continuum of scattered states. However, upon a closer look, one should recognize in  $v$  the imaginary part of the Bethe ansatz wave function. Then it is clear that at the crossing point  $v = 0$  and a continuous solution is allowed if  $v$  becomes imaginary above the crossing point. This corresponds to an oscillating, delocalized amplitude of a scattered two-magnon state. With this in mind, one can easily verify that Bethe's equations share the same behaviour. Thus, the distinction between bound and scattered states on a discrete lattice consists not in their energy but in the behaviour of the wave function. The physical reason for the decay is the vanishing of magnon-magnon attraction precisely at the borderline of the continuum where the crossover from localized (bound) to delocalized (scattered) states takes place. We can also see that by increasing the number of spins the energies of the two eigenmodes merge so fast that one could hardly distinguish them already at modest values of  $N$ . For the Bethe ansatz equations the exact  $1/N$ -expansion was considered before and in the long-wave region of the spectrum the so-called non-string solutions were obtained [10,11]. In contrast to the string solutions which describe odd and even excitations, only the even ones are allowed to exist for momenta  $P \lesssim 1/\sqrt{N}$ . Our approximation agrees well with this picture (see a more detailed analysis in [3]), but, as an approximation, it, of course, slightly deviates from the exact expansion. It can also be seen that, if the solution for the Fourier amplitude is substituted into the continuum version of (3), one does not reproduce the exact result for the  $N \rightarrow \infty$  limit (for a recent review of Bethe's ansatz see [12]). The proper analytical continuation from a discrete lattice to continuum ( $X \rightarrow x$ ) can be achieved by explicitly introducing the symmetry requirements into the

amplitude:  $A_{s,a}(x) = \frac{1}{2}(a_{a,s}(x) \pm a_{a,s}(N-x))$ . Normalization constants are then readily obtained and we get the correct result which agrees with the Bethe ansatz at  $N \rightarrow \infty$ :  $A_{s,a}(x) = \frac{\sin(\frac{p}{2})}{\sqrt{2}} [\cos^{x-1}(\frac{p}{2}) \pm \cos^{N-x-1}(\frac{p}{2})]$ . In the discrete case the allowed values of the total momentum required to excite one or another bound state are distributed in an alternate order over the Brillouin zone. The most probable location of the two overturned spins for both modes is at the nearest-neighbour sites,  $x = 1$  and  $x = N - 1$ . We can see from the above expression that the reason for the instability of the antisymmetric state resides in the vanishing of its amplitude at large separation of the overturned spins ( $\sim N/2$ ), *i.e.* this state is more loosely bound.

We turn now to a more challenging 2D case where our formalism opens new perspectives to study the excitations. Apparently, one should not expect the finite-size effects to be larger than for the 1D chain and therefore assume an even faster convergence to the two energy branches found by Wortis [6]. However, it turns out that not all the new modes we find for the square lattice follow this tendency. On the contrary, some of them stay well separated in energy from all the others and could be easily observed even at macroscopic values of  $N$ . Existence of different types of excitations follows from the symmetry relations (2) depending on the parity of the quantum numbers  $l_x$  and  $l_y$  and also from the symmetry group  $C_{4v}$  of the lattice. The excitation modes should transform according to the irreducible representations of the group and their classification is obtained by using the projection operator  $\hat{O}_\alpha$  (see, *e.g.*, [13]). For a fixed momentum  $\mathbf{P}$  the action of  $\hat{O}_\alpha$  on the Fourier expansion (3) projects out a function which transforms according to one of the five irreducible representations  $\alpha$  of the group: four one-dimensional representations  $A_1$ ,  $A_2$ ,  $B_1$  and  $B_2$  and one two-dimensional  $E$ . Our convention of numbering the lattice sites should be taken into account when describing the group transformations. For instance, the  $C_4$  rotation gives  $C_4(X, Y) \rightarrow (N - Y, X)$ . There are three different combinations of the quantum numbers: 1) both  $l_x$  and  $l_y$  are even, 2) both  $l_x$  and  $l_y$  are odd, 3) the numbers are of different parity. These combinations determine the respective sequences for  $\mathbf{Q}$  in (3). The projection operator then generates the modes allowed for a particular combination. Thus, we find that only 2 modes “survive” the projection for the first combination of quantum numbers:  $A_1$  and  $B_1$ . The second combination allows  $A_2$  and  $B_2$  and the third one corresponds to the  $E$  mode. It has to be noted that due to their association to odd quantum numbers the “strange”  $A_2$  and  $B_2$  modes are different by symmetry from the standard ones (*e.g.*,  $B_2$  transforming as  $XY$ ) which would arise for both  $l_x$  and  $l_y$  even, unless being forbidden by the symmetry of the lattice. Thus we get

$$\begin{aligned} a_{A_1, B_1}(X, Y) &= \frac{1}{2N^2} \sum_{Q_x^s, Q_y^s} b_{A_1, B_1}(Q_x, Q_y) \times (\cos(Q_x X) \cos(Q_y Y) \pm Q_y \longleftrightarrow Q_x), \\ a_{A_2, B_2}(X, Y) &= \frac{1}{2N^2} \sum_{Q_x^a, Q_y^a} b_{A_2, B_2}(Q_x, Q_y) \times (\cos(Q_x X) \cos(Q_y Y) \mp Q_y \longleftrightarrow Q_x), \\ a_E(X, Y) &= \frac{1}{N^2} \sum_{Q_x^a, Q_y^s \text{ or } Q_x^s, Q_y^a} b_E(Q_x, Q_y) \times \begin{pmatrix} \cos Q_x Y \cos Q_y X \\ \cos Q_x X \cos Q_y Y \end{pmatrix}. \end{aligned} \quad (6)$$

When these expressions are substituted into eq. (1), one obtains a  $2 \times 2$  matrix generalization of the eigenproblem. According to our continuum treatment of the 1D case, we replace the double sums by double integrals which keep track of the finite size via respective boundaries of integration. The amplitudes are obtained after the proper continuation from the discrete lattice as described above. We then find that the  $A_1$  and  $B_1$  modes should be identified with the two eigenenergy solutions found before [6, 7]. The  $A_1$  mode is stable for the whole Brillouin zone and has the lowest energy as compared to the other modes. The  $B_1$  mode, the highest in

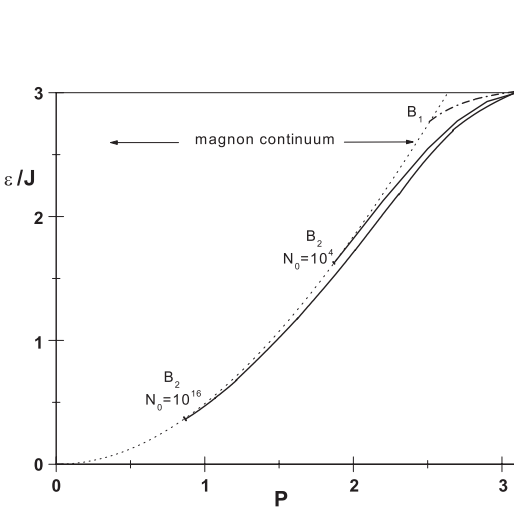


Fig. 1

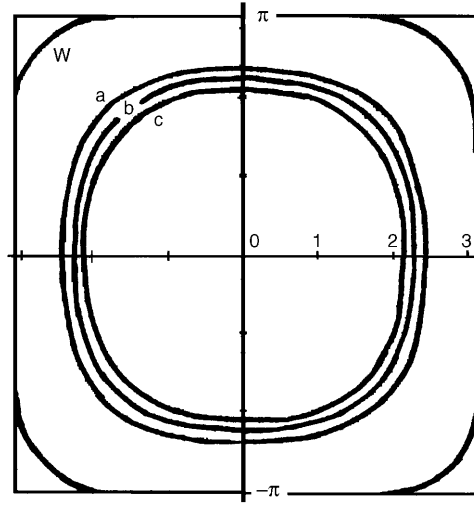


Fig. 2

Fig. 1 – Dispersion of the  $B_2$  mode along the diagonal direction  $p_x = p_y$  for the two values of the number of spins  $N_0$  as determined from our approximation. The dispersion of the  $B_1$  mode was obtained by Wortis in [6].

Fig. 2 – Critical lines defining the regions of stability (area outside the respective line) for the  $B_2$  mode. The line “a” corresponds to our coarse approximation, “b” to the improved one (incorporating the exact 1D solution) and “c” to the numerical calculations for  $N_0 = 10^4$ . The line “W” is independent of  $N$  and stands for the  $B_1$  mode.

energy, has a very narrow and anisotropic region of stability mostly concentrated around the corners of the zone. For instance, along the diagonal direction ( $p_x = p_y = p$ ) we get the same analytical value as in [6] for the critical momentum  $p_c^{B_1} = 2 \arccos(\frac{4}{\pi} - 1)$ , marking the crossing point with the lower boundary of the continuum of scattered states,  $E_L = 2J(2 - \cos(p_x/2) - \cos(p_y/2))$ . The four new modes are obtained from the  $N$ -expansion of the corresponding integrals containing the cutoffs. After straightforward calculations we find that the energies of the  $A_2$ -mode and one of the components of the  $E$ -mode lie close within the  $J/(N \ln N)$  range correction to the energy of the  $B_1$  mode and thus their  $N$ -dependence is negligible (the  $p_x = p_y$  direction is chosen). The most dramatic is the behaviour of the  $B_2$  mode (and similarly, of the other component of the  $E$  mode) whose dispersion evolves from being close to that of the  $B_1$  towards the  $A_1$  mode by increasing the number of spins as illustrated in fig. 1.

Due to the logarithmic  $N$ -dependence of its energy, the  $B_2$  mode is well separated from the reference  $A_1$  and  $B_1$  branches. This separation becomes most prominent for a mesoscopic system when the branch is “half-way” between the two modes above. At a local scale the shape of  $a_{B_2}(X, Y)$  approaches that of the  $A_1$  mode by increasing the number of spins. We have also carried out numerical calculations of the solutions of eq. (1) for not very large values of  $N$  which confirm these unexpected findings.

An important improvement of our approximate description of a mesoscopic ferromagnet can be achieved if an exact solution for 1D is incorporated in the formalism. The functional form of the Bethe ansatz does not lend itself easily to this purpose—an observation which may explain why Bethe’s original hope to reach out for higher dimensions did not materialize [4]. The alternative we propose is based on new formulas for finite lattice summation (details of

derivation will be given elsewhere). In particular, we find a new form for the exact solution of Bethe's bound-state problem without making an ansatz:

$$\begin{aligned} a_a(X) &= \frac{C_a}{N} \sum_{k=0}^{N-1} \frac{\cos\left(\left(\frac{2\pi}{N}k + \frac{\pi}{N}\right)X\right)}{\cosh(v) - \cos\left(\frac{2\pi}{N}k + \frac{\pi}{N}\right)} = C_a \frac{\tanh\left(\frac{Nv}{2}\right) \cosh(Xv) - \sinh(Xv)}{\sinh(v)}, \\ a_s(X) &= \frac{C_s}{N} \sum_{k=0}^{N-1} \frac{\cos\left(\left(\frac{2\pi}{N}k\right)X\right)}{\cosh(v) - \cos\left(\frac{2\pi}{N}k\right)} = C_s \frac{\coth\left(\frac{Nv}{2}\right) \cosh(Xv) - \sinh(Xv)}{\sinh(v)}, \end{aligned} \quad (7)$$

where  $\cosh(v) = (1 - \varepsilon/2J)/\cos(\frac{P}{2})$ ,  $X \in [0, N-1]$  and  $C_{a,s}$  are the normalization constants which can easily be obtained by using the general formulas above. Then  $v$  can be identified with the imaginary part of the Bethe ansatz phase  $\theta$  as noted above and one easily obtains Bethe's eigenenergy equation if the wave function (7) is substituted into (1). However (7) represents a more general exact relation where  $v$  is an arbitrary complex variable, implying that it can also be used to describe the scattered magnon continuum. More importantly, (7) can now be directly introduced in our continuum approach by reducing the number of integrals. The  $N$ -expansion we obtain in this way turns out to be both closer to numerical calculations and easier to obtain analytically. For instance, one can compare the expression defining the critical point ( $p_x^c = p_y^c = p_{B_2}^c$ )

$$2\left(1 - \cos\left(\frac{p_{B_2}^c}{2}\right)\right) \simeq \frac{1}{\frac{1}{\pi} \ln N - 0.22}$$

of the initial approximation with the improved one

$$2\left(1 - \cos\left(\frac{p_{B_2}^c}{2}\right)\right) \simeq \frac{1}{\frac{1}{\pi} \ln N - 0.04}.$$

The numerical calculation for  $N = 100$  gives  $p_{B_2}^c = 1.54$ , while from the above expressions we get 1.86 and 1.73, respectively. Figure 2 shows the critical lines for the  $B_2$  mode calculated by using both the coarse and the improved approximation as well as the result of numerical calculation for  $N = 100$ . Another result of calculations is that the critical lines above are converging with increasing  $N$ . This implies that our approximation captures correctly the main term of the  $N$ -expansion for the exact solution.

We conclude that although the problem of bound magnon excitations in the ferromagnetic Heisenberg model was considered completely solved long time ago, our approach has allowed to find several new modes and describe the distribution of bound states over the Brillouin zone. Contrary to expectation some of the new modes remain well separated from the others even at macroscopic values of  $N$ . These "mesoscopic" modes increase their stability with increasing the number of spins. Obviously, similar features can be found in multimagnon spectra too. The continuum approach presented above provides new reliable approximations for finite systems and can be extended to other models too.

\* \* \*

Financial support from the Concerted Action Scheme of the Flemish Government and from the National Science Foundation (FWO) is gratefully acknowledged. One of us, SC, also acknowledges support from the Supreme Council for Scientific and Technological Development of Moldova.

## REFERENCES

- [1] Spin effects in mesoscopic systems: *Solid State Commun.*, **119** (2001) Issue 4-5.
- [2] HENELIUS P., SANDVIK A. W., TIMM C. and GIRVIN S. M., *Phys. Rev. B*, **61** (2000) 364.
- [3] CEULEMANS A., COJOCARU S. and CHIBOTARU L. F., *Eur. Phys. J. B*, **21** (2001) 511.
- [4] BETHE H., *Z. Phys.*, **71** (1931) 205.
- [5] FUKUDA N. and WORTIS M., *J. Phys. Chem. Solids*, **24** (1963) 1675.
- [6] WORTIS M., *Phys. Rev.*, **132** (1963) 85.
- [7] HOOD M. and LOLY P. D., *J. Phys. C*, **19** (1986) 4729.
- [8] MATTIS D. C., *The Theory of Magnetism*, Vol. **I** (Springer Verlag, Berlin, Heidelberg) 1981, p. 300.
- [9] IZYUMOV YU. A., SKRIABIN YU. N. and COOKER R., *Statistical Mechanics of Magnetically Ordered Systems* (Consultants Bureau, New York) 1988, p. 295.
- [10] WOYNAROVICH F., *J. Phys. A*, **15** (1982) 2985.
- [11] VLADIMIROV A. A., *Phys. Lett. A*, **105** (1984) 418.
- [12] KARBACH M. and MÜLLER G., *Comput. Phys.*, **11** (1997) 36.
- [13] ELLIOT J. P. and DAWBER P. G., *Symmetry in Physics*, Vol. **I** (The Macmillan Press Ltd, London) 1979, p. 360.